

## Green's Function Retrieval from the CCF of Random Waves and Energy Conservation for an Obstacle of Arbitrary Shape

Haruo Sato<sup>1\*</sup>

<sup>1</sup>Tohoku university, Science, Geophysics

For imaging the earth structure, the cross-correlation function (CCF) of random waves as ambient noise or coda waves has been widely used for the estimation of the Green's function. Here we study the mathematics of the Green's function retrieval in relation to the energy conservation for a single obstacle of arbitrary shape. When an obstacle is placed in a 2-D homogeneous medium, the Green's function is written by a double series expansion using Hankel functions of the first kind which represent outgoing waves. When two receivers and the scattering obstacle are illuminated by uncorrelated noise sources randomly and uniformly distributed on a closed circle of a large radius surrounding them, the lag-time derivative of the CCF of random waves at the two receivers can be written by a convolution of the anti-symmetrized Green's function and the auto-correlation function of the noise source time function. We explicitly derive the constraint for the Hankel function expansion coefficients as the sufficient condition for the Green's function retrieval. We show that the constraint is equivalent to the generalized optical theorem derived from the energy conservation principle. Physical meaning of the generalized optical theorem becomes clear when the Hankel function expansion coefficients are transformed into scattering amplitudes in the framework of the conventional scattering theory.

Sato, H. 2013. Green's Function Retrieval from the CCF of Random Waves and Energy Conservation for an Obstacle of Arbitrary Shape: Noise Source Distribution on a Large Surrounding Shell, *Geophys. J. Int.* in press.

Keywords: Seismic waves, Scattering, structure study, Green function, wave theory

## Characteristics of the CCF of coda waves: dependence on the angle between the station pair and the source

Kentaro Emoto<sup>1\*</sup>, CAMPILLO, Michel<sup>1</sup>, BRENGUIER, Florent<sup>1</sup>, BRIAND, Xavier<sup>1</sup>, Tetsuya Takeda<sup>2</sup>

<sup>1</sup>ISterre, University of Grenoble, France, <sup>2</sup>NIED

Coda of earthquakes consists of scattered waves and the late coda can be regarded as a diffuse field. The diffuse wave field is necessary for the seismic interferometry. Campillo & Paul (2003) showed that we can extract the Green's function from field-to-field correlation of coda waves. Different from the noise field, scattered waves around the source region are included in the coda. We analyze the cross-correlation functions (CCF) of coda of earthquakes occurred around the source region of the 2011 Tohoku-oki earthquake and examine the fluctuation of them.

We use the earthquakes with magnitude larger than 5 occurred from 2008 to 2011 and about 74 Hi-net stations located in the east coast of northeastern Japan. We apply the band-pass filter (0.1 - 0.2Hz) and divide the coda window into 300s-long segments from 200s after the origin time until 700s with an interval of overlap of 100s. By stacking the CCFs, we detect the Rayleigh wave with the propagation velocity of 3.2km/s. We examine the dependence on the source location by using the angle between the source and the station pair. The CCFs with angles less than 45 degrees are asymmetry. On the other hand, the CCFs with the angles larger than 45 degrees are more symmetric. This feature was also reported in Paul et al. (2005). This observation indicates that the energy coming from the source is still dominant in the late coda.

We calculate the fractional travel-time change,  $dt/t$ , by applying the stretching method to the coda of the CCF and analyze the fluctuation of it. The  $dt/t$  shows the strong fluctuation and the RMS of it is about a few percent. This fluctuation is not systematic. The fluctuation of the  $dt/t$  measurement based on the stretching method due to the random fluctuation of the waveform is theoretically estimated by Weaver et al (2011). When we apply their theory to our measurement, the predicted fluctuation and the observed fluctuation are the same order of magnitude. This result indicates that the observed fluctuation of  $dt/t$  is not reflected the uniform change of the medium. Because the diffuse field of coda is not isotropic, we can't obtain the stable CCF from the coda. We also calculate the CCF of noise field in the same region and calculate the  $dt/t$  due to the 2011 Tohoku-oki earthquake by applying the stretching method. We observe the co-seismic change of  $dt/t$ . The  $dt/t$  increases by about 0.2 % after the earthquake. This is one order of magnitude smaller than the fluctuation of  $dt/t$  derived from the CCF of coda. Therefore we can't detect the change due to the earthquake from the CCF of coda. In order to improve the stability of the CCF of coda, we apply the curvelet denoising filter (Stehly et al 2011). By the denoising, the correlation coefficient between each CCF and the stretched reference CCF increases and the fluctuation of the  $dt/t$  decreases. However, the fluctuation is still too large to detect the co-seismic change.

Finally, we mention about the signal to noise ratio (SNR) of the CCF. The SNR of the CCF of noise is about 3 times larger than that of the CCF of coda. The ratio of the square root of the length of the time window of the noise used to calculate the one-day CCF to that of the coda is about 14. Therefore, in terms of the length of the time window, the CCF of the coda is efficient to extract the Green's function compared with the noise.

Keywords: Coda wave, Seismic interferometry

## Theoretical background for estimating attenuation structures with seismic interferometry

Hisashi Nakahara<sup>1\*</sup>

<sup>1</sup>Hisashi Nakahara

Seismic interferometry or the noise correlation method has provided passive methods for travel time tomography. However, it is not clear yet whether amplitudes of Green's functions retrieved from cross correlations can be reliably used to estimate attenuation. Recently, an equation was conjectured by Prieto et al. (2009), which is thought to be an extension of the SPAC method (e.g. Aki, 1957) to lossy media, and it was used to estimate attenuation structures from amplitudes of the retrieved Green's functions. However, the conjecture is not clearly proved yet though numerical and analytical studies are being made. In this study, I prove a theoretical relation between the SPAC method and seismic interferometry for heterogeneous lossy media, and then develop a theory to support the conjecture by the help of the relation. The conjecture turns out to be derived for homogeneous lossy media under two assumptions of (1) weak attenuation and (2) larger station separations than a considered wavelength. Based on the results, applications of seismic interferometry to the estimation of attenuation should be conducted in relatively homogeneous regions with weak attenuation. Applications to attenuation tomography in heterogeneous regions still need to be investigated theoretically.

### Acknowledgments

This study was partially supported by JST J-RAPID program.

Keywords: seismic interferometry, SPAC method, attenuation

## Seismic interferometric reverse time migration to passive seismic data for subsurface structural survey

Kazuya Shiraishi<sup>1\*</sup>

<sup>1</sup>JGI, Inc.

In this study, I propose an imaging method, SI-RTM, for a direct subsurface imaging from passive seismic data by implementing the reverse time migration (RTM) with a concept of the seismic interferometry (SI). The RTM based on a two-way wave equation is a powerful imaging technique in reflection seismic survey for complex subsurface structures, while it takes higher computational cost than conventional migration methods. The RTM principle is represented an imaging condition that the reflected or scattered waves are focused on the imaging points by time integrating the product of two extrapolated wavefields at same recording time; the forward extrapolated wavefield of source wavelet from a source point and the backward extrapolated wavefield of the recorded seismic data from receiver points. The SI is generally used for a redatuming or a signal extraction by crosscorrelating the different seismic traces in a data domain, then the synthesized waveforms are analyzed for wavefield characterization or processed for the subsurface imaging.

The SI-RTM could be recognized as a wavefield interference in an image domain. Instead of the wavefield extrapolation in the conventional RTM, arbitrary time-windowed seismic record is propagated forwards from a receiver point which become a virtual source and is propagated backwards from other receiver points. If any multiple reflecting waves between the surface and the reflection boundaries satisfy the imaging condition, the reflected energy will be focused on subsurface reflection points. The imaging process corresponds to the wavefield extrapolation with a velocity model and interference in the image domain simultaneously. In this study, I evaluated the SI-RTM algorithm by a two-dimensional numerical simulation. Two kinds of synthetic passive seismic data were generated by a finite difference elastic wave modeling; (a) local earthquakes data, and (b) ambient seismic noise data which contain body waves randomly generated. The SI-RTM was implemented under acoustic wavefield condition. Both the test results show validity of the imaging algorithm of SI-RTM.

The SI-RTM needs a velocity model for wavefield extrapolation and takes high computational cost which is dependent on the data volume and the size of a target area. However, it enables us to achieve the direct seismic imaging without source information, and it improves analysis method of the passive seismic data by not only the SI record synthesized in the data domain but also the SI profiles in the image domain when it is difficult to recognize the significant phase on the SI virtual source record. In the engineering aspect, this method will contribute to beneficial use of the passive seismic data in any monitoring projects. In the future work, realistic problems will be overcome by continuing field data study, including further applications such as the imaging of multi-component passive seismic data.

Keywords: reverse time migration, seismic interferometry, passive seismic, reflection seismic survey, numerical simulation

## Time-lapse changes in velocity and anisotropy after the 2011 Tohoku earthquake estimated by seismic interferometry

Nori Nakata<sup>1\*</sup>, Roel Snieder<sup>1</sup>

<sup>1</sup>Colorado School of Mines

Seismologists have estimated time-lapse changes in subsurface velocities and anisotropy caused by the 2011 Tohoku earthquake for two years. Seismic interferometry is recognized as a powerful tool to monitor the velocities and anisotropy, and applied to earthquake records and ambient-noise data recorded by KiK-net, Hi-net, and other seismometers. We apply seismic interferometry to KiK-net data and estimate mean values of near-surface shear-wave velocities in the periods of January 1–March 10 and March 12–May 26 in 2011. We detect about a 5% reduction in the velocity after the Tohoku earthquake. The area of the velocity reduction is about 1,200 km wide, which is much wider than earlier studies reporting velocity reductions after larger earthquakes. The reduction partly recovers with time. We can also estimate the azimuthal anisotropy by detecting shear-wave splitting after applying seismic interferometry. Estimating mean values over the same periods as the velocity, we find the strength of anisotropy increased in most parts of northeastern Japan, but fast shear-wave polarization directions in the near surface did not significantly change. The changes in anisotropy and velocity are generally correlated, especially in the northeastern Honshu (the main island in Japan).

Keywords: seismic interferometry, Tohoku earthquake, time lapse, shear-wave velocity, shear-wave splitting, KiK-net

## Computer simulation of high-frequency Po/So propagation in the oceanic lithosphere

Takashi Furumura<sup>1\*</sup>, BLN Kennett<sup>2</sup>

<sup>1</sup>CIDIR/ERI Univ. Tokyo, <sup>2</sup>RSES ANU

The phases Po/So are very distinctive high-frequency signals travelling often more than 1000-3000 km through the oceanic lithosphere and recorded at the ocean bottom seismographs with a long coda. We demonstrate that such Po/So signals are developed by multiple forward scattering of high-frequency body P and S wave in heterogeneous oceanic lithosphere based on the analysis of observed set of waveforms and finite-difference simulation of high-frequency seismic wave propagation in heterogeneous structures.

An important component of the propagation is provided by reverberation in the water column and sediments linked to P and S propagation in the oceanic lithosphere. The nature of the observed Po and So phases with high frequencies and long coda is well represented by multiple forward scattering in a lithospheric structure with and quasi-laminate heterogeneity with horizontal scales much larger than vertical.

Despite the generally good propagation of Po/So to stations in the western Pacific such as from the Japan subduction zone to the Wake island ocean bottom stations near Tonga, the propagation in eastern Pacific, e.g., to the H2O station on an old telephone cable between Hawaii and the mainland USA is rather poor for So (Kennett, Zhao and Furumura, 2009). Such poor transmission of the high-frequency Po/So signals along the young (< 25 Ma) oceanic plate can be explained by the ineffective propagation of high-frequency signals in a thinner lithosphere with influence also from oblique propagation across major transform fault systems in the eastern Pacific with changes in lithospheric thickness.

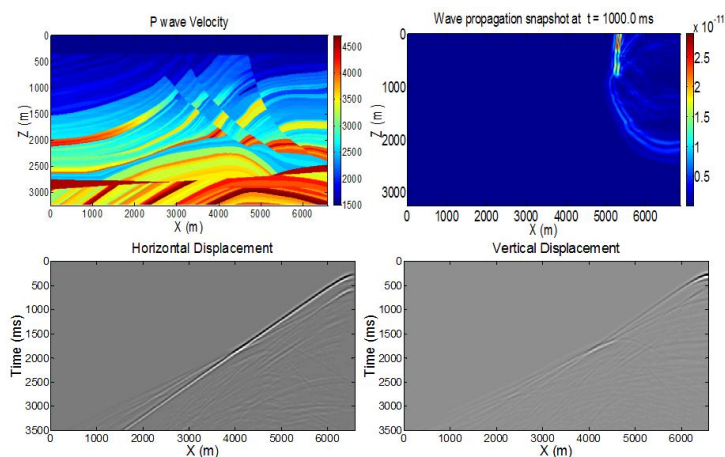
## Elastic waveform modeling in frequency domain with an efficient MATLAB code

Ehsan Jamali Hondori<sup>1\*</sup>, Hitoshi Mikada<sup>1</sup>, Tada-nori Goto<sup>1</sup>, Junichi Takekawa<sup>1</sup>

<sup>1</sup>Graduate School of Engineering, Kyoto University

Seismic waveform modeling is a key tool to estimate subsurface characteristics, not only for hydrocarbon explorations but also for proper managements of seismic hazards and civil engineering infrastructures. Modeling in frequency domain found to be effective for its numerous advantages compared to that in time domain. Once triangular factors of impedance matrix have been calculated, multiple sources can be processed with the minimum computational costs. Monochromatic and band limited modeling at desired frequencies are implemented in a straightforward manner and the attenuation behavior of elastic media can directly be dealt with considering complex valued elastic parameters. However, discretizing the computational domain requires more grid points to achieve acceptable accuracy and a program with robust algorithm is needed to minimize the modeling time and cost. We used 25-point finite difference stencils to discretize the elastic wave equation in frequency domain to develop an effective MATLAB package for elastic waveform modeling. By using array-processing abilities of MATLAB, we efficiently computed the large impedance matrix for realistic model sizes. In order to solve the system of equations impedance matrix is factorized to lower and upper triangular matrixes, then forward and backward substitution results in horizontal and vertical displacements. Since the impedance matrix has a band structure and very sparse pattern, using efficient ordering schemes to reduce fill-in during factorization is necessary. We used METIS library together with SuiteSparse library for sparse LU factorization. METIS uses a multilevel nested dissection algorithm to calculate a fill reducing ordering which brings a superior performance to the program. SuiteSparse includes several factorization and solution modules, such as UMFPACK, SparseQR, and CHOLMOD, for sparse matrixes and linear system of equations. We used UMFPACK and SparseQR modules in our modeling code for problems with different sizes. Once the factors have been calculated, several seismic sources could be modeled by solving for multiple right hand sides. Reflections from truncated boundaries appear in the solution of the wave equation which must be suppressed by boundary conditions. In order to truncate the computational area we applied Perfectly Matched Layers (PML) on the boundaries. Complex valued velocities based on Kolsky-Futterman model were used to consider attenuation effects in the seismic waveforms. Marmousi2 example (Figure 1) confirmed the efficiency and accuracy of the MATLAB code. We have cropped the original model to focus on the more complex area in the center of the geological model; the final model in the example is 6600 m long and 3200 m deep. A snapshot of wave propagation and shot gathers of horizontal and vertical components of the displacement recorded at the surface are shown in the Figure 1. As is obvious in the horizontal displacement component, strong Rayleigh waves appear in the seismograms and travel near surface with low velocity. Based on the results of Marmousi2 example and several other models which have already tested the program, the developed MATLAB package can be used for fast and accurate elastic waveform modeling.

Keywords: seismic, waveform modeling, frequency domain, finite difference, perfectly matched layers



## Amplitude distribution of sP reflected phase from offshore earthquakes in the Pacific side of Tohoku district

Masahiro Kosuga<sup>1\*</sup>

<sup>1</sup>Graduate School of Sci. and Tech., Hirosaki Univ.

We observed a prominent phase on vertical seismograms of interplate and intraplate earthquakes offshore Miyagi prefecture with depth ranges from 30 to 60 km. The phase that appears between P- and S-waves is observed widely at stations in the Japan Sea side. Here we examine the waveform and travel times of this phase using Hi-net data and estimate its origin, and discuss potential usage of the phase.

A polarization analysis indicates that the phase has a strike toward the epicenter, nearly vertical dip angle, and large rectilinearity. This indicates that the phase is P-wave coming from the direction of the source. The travel time of the X-phase is proportional to epicentral distance with an apparent velocity of about 7 km/s. This suggests that the reflection/conversion occurs at relatively shallow part. There is no significant azimuthal variation in arrival times of the X-phase, which implies that the plane of reflection/conversion is nearly horizontal. We estimate the position of conversion/reflection by using ordinary hypocenter location method assuming that the phase is P-wave from the conversion/reflection point. The location is near the surface of the coastal area of Miyagi prefecture. The above observational facts of large amplitude, polarization characteristics, apparent velocity, azimuthal variation of arrival times, and the location of conversion/reflection point, are all consistent with an interpretation that the phase is sP reflected phase from the surface. This phase has already found by previous studies and has been used as a depth phase to improve the depth accuracy in hypocenter location and delineate a seismicity pattern along the plate boundary.

Next we investigated amplitude distribution of sP phase. We measured amplitude on RMS envelope as the deviation of smoothly varying envelope. In many cases the amplitude is largest at stations in Akita and Yamagata prefectures, while the amplitude is smaller at stations in the northern and southern part of Tohoku district, and at stations in the Pacific side. The focal mechanisms of these events are reverse faulting with N-S strike. In the case of reverse faulting earthquake with E-W strike, the area of large amplitude shifts to the northern part of Tohoku district. This indicates that the amplitude distribution of sP phase depends on focal mechanisms. Thus the amplitude of sP phase has a potential usage to determine focal mechanisms of offshore earthquakes, which is difficult from the P-wave polarization only.

Acknowledgement: We thank the National Research Institute for Earth Science and Disaster Prevention (NIED) for providing waveform data from Hi-net.

Keywords: sP wave, reflection, amplitude, focal mechanisms

## Effect of brine viscosity on ultrasonic wave attenuation

Jun Matsushima<sup>1\*</sup>

<sup>1</sup>The University of Tokyo

Seismic attenuation is a highly variable physical parameter that depends on confining pressure, porosity, degree of fluid saturation, and variations in fluid properties such as elastic modulus, viscosity, and polarity. In our previous paper, we used partially frozen brine as a solid-liquid coexistence system to investigate seismic attenuation phenomena. Ultrasonic wave transmission measurements on this ice-brine coexisting system were conducted to examine the influence of unfrozen brine in the pore microstructure of ice on ultrasonic waves. From liquid phase to around the freezing point, the presence of a partially frozen brine increases both velocity and attenuation. During the growth of ice from brine, salt cannot incorporate into the ice crystals. As the ice freezes, the salt is rejected and concentrates in the brine; thus, as the salinity increases in the brine filled pores, the freezing point of the remaining fluid is successively lowered and furthermore the viscosity of remaining high salinity unfrozen brines becomes larger and larger. Seismic attenuation related to viscous effect is caused by relative fluid-solid motion is one of the most important attenuation mechanisms. This paper is concerned with the effect of such viscosity on attenuation at ultrasonic frequencies. We observed the variations of a transmitted wave, changing its salinity and quantitatively estimated attenuation for unconsolidated porous material saturated with brine by considering different distances between the source and receiver transducers. The waveform analyses for P-waves indicate that the attenuation increases with increasing salinity (i.e. increasing viscosity). In order to elucidate the physical mechanism responsible for ultrasonic wave attenuation measured at different salinity (i.e. different viscosity), we employ a poroelastic model based on the Biot theory to describe the propagation of ultrasonic waves through partially frozen brines.

Keywords: Seismic attenuation, viscosity, poroelastic

## Characteristics of high-frequency seismic waves during relatively deep event at Kanto region

Shunsuke Takemura<sup>1\*</sup>, Kazuo Yoshimoto<sup>1</sup>

<sup>1</sup>Yokohama City University

### Observed Characteristics of high-frequency seismic waves

Observed records during Mw 5.0 earthquake occurring at depth of 53 km at southwestern Ibaraki, central part of Japan, demonstrated various features depending on the station location. Especially, the waveforms with 2-4 Hz at central and southern part of Chiba are showing strong peak delay and spindle shape of S wave, while weak peak delay appears at other area in Kanto region. In the high frequency ( $f > 1$  Hz), seismic waves are strongly affected by the effect of seismic wave scattering due to small-scale velocity fluctuation along propagation path (e.g. Sato, 1989). The spatial distribution of small-scale velocity fluctuation in the subsurface structure of Kanto area may be cause of strong peak delay (e.g., Takahashi et al., 2007).

### 2-D FDM simulation

We conduct FDM simulation of seismic wave propagation in the 2-D heterogeneous structure to clarify the cause of strong peak delay. Our 2-D simulation model is covering the zone 245 by 123 km, which has been discretized with grid size 0.015 km. We assume the layered background velocity structure base on the model proposed by Koketsu et al. (2008). The model is including basin structure, crust, mantle and subducting oceanic plate.

In order to introduce the effect of seismic wave scattering, we assume stochastic random velocity fluctuation in each layer. Random velocity fluctuations are characterized by exponential-type auto-correlation function (ACF) with correlation distance  $a = 3$  km and strength of fluctuation  $e = 0.05$  in the upper crust,  $a = 3$  km and  $e = 0.07$  in the lower crust,  $a = 10$  km and  $e = 0.02$  in the mantle (e.g., Takemura and Furumura, 2013). In the subducting plate, we assume anisotropic random velocity fluctuation characterized by exponential-type ACF with  $a_H = 10$  km in horizontal direction,  $a_Z = 0.5$  km in vertical direction and  $e = 0.02$  (Furumura and Kennett, 2005). In the low velocity layer, basin structure, we assume random velocity fluctuation model characterized by exponential-type ACF with  $a = 1$  km in vertical direction and  $e = 0.07$ .

In addition, we assume the low-velocity zone at northeastern part of Chiba with depth of 30 km (Matsubara et al., 2004). In the low-velocity zone, random velocity fluctuation characterized by Gaussian-type ACF with  $a = 0.5$  km and  $e = 0.10$  is superposed on exponential-type ACF with  $a = 3$  km and  $e = 0.07$ . Strong seismic scattering would occur in the low-velocity zone of simulation model and affect peak delay time at Chiba.

### Simulation results

Simulated waveforms with 2-4 Hz are showing spindle shape due to scattering and energy trap in the basin structure. Strong peak delay also appears at central and southern part of Chiba. Simulation result demonstrated that strong scatters in the low velocity zone play important role in peak delay time and waveform shape.

Low-velocity zone at northeastern Chiba is considered as a result of dehydrated water from oceanic crust of subducted Philippine Sea plate. Therefore strong small-scale velocity fluctuation in the low-velocity zone may be related with dehydrated water.

### Acknowledgement

We acknowledge the National Research Institute for Earth Science and Disaster Prevention, Japan (NIED) for providing the K-NET/KiK-net waveform data. The computations were conducted on the Earth Simulator at the Japan Marine Science and Technology Center (JAMSTEC).

Keywords: seismic wave, numerical simulation, seismic wave scattering, heterogeneous subsurface structure

## Tsunami-induced ground tilt changes observed by Hi-net and F-net in Japan

Takeshi Kimura<sup>1\*</sup>, Sachiko Tanaka<sup>1</sup>, Tatsuhiko Saito<sup>1</sup>

<sup>1</sup>National Research Institute for Earth Science and Disaster Prevention

Oscillating ground tilt perturbations accompanied by the 2010 Maule, Chile, earthquake tsunami were observed over a broad inland area facing the Pacific Ocean coast in Japan by high-sensitivity accelerometers of Hi-net (Kimura et al., 2013, JGR) and broadband seismometers of F-net. In the present study, we investigated the characteristics of the ground tilt changes induced by the Maule earthquake tsunami using the Hi-net tiltmeter records. The very dense network throughout Japan revealed the precise distribution of the tsunami-induced perturbations. To demonstrate the link between the tsunami and the observed inland tilt changes, we also simulated the deformation of the solid Earth due to the ocean loading disturbances caused by the tsunami. Furthermore, based on our observations and a simple tsunami model, we discussed possible uses of land data in characterizing tsunami behavior, particularly in nearshore environments.

Through an analysis of ground tilt data observed at more than 500 Hi-net stations, we were able to obtain a detailed spatiotemporal distribution of the tsunami-induced tilt changes and reveal a relationship between the tilt amplitude and the distance from the coast. At distances of 1 km or less, the peak tilt amplitudes were  $\sim 5 \times 10^{-8}$  rad and were almost constant with respect to the distance. At distances greater than 3 km, amplitudes were inversely proportional to the distance and reached  $\sim 5 \times 10^{-9}$  rad approximately 50 km away from the coast. The dominant ground tilting directions were almost the same as the direction orthogonal to the coastline. The tsunami-induced signals were also observed at F-net stations in coastal area and small islands.

These observed ground tilt changes and their characteristics were successfully modeled with a loading deformation caused by sea level variations accompanied by the tsunami. Applying a two-dimensional boxcar tsunami model to the observed data, we estimated the water volume per unit length of coast for the Maule earthquake tsunami to be  $2-7 \times 10^3 \text{ m}^3/\text{m}$  within the distance of 14-20 km seaward of the coastline.

## Tsunami generation and propagation due to sea-bottom deformation: A linear potential theory

Tatsuhiko Saito<sup>1\*</sup>

<sup>1</sup>NIED

The present study obtained a solution of the velocity potential for sea-bottom deformation with an arbitrary source time function for constant water depth. By using this velocity potential, we theoretically derived semi-analytical solutions of the velocity distributions in the sea, the water height at the surface, and the pressure at the bottom. The velocity distribution is represented by the sum of the direct and indirect components excited from the sea-bottom deformation: the direct component is the velocity distribution excited directly from the sea-bottom deformation and the indirect component the velocity distribution excited from the water height distribution at the surface. The semi-analytical solution indicates that the direct component should be zero or the initial velocity distribution be zero as the initial condition for 2-D tsunami propagation simulations. The pressure at the bottom is represented by the sum of hydrostatic and dynamic components. When the sea-bottom uplifts with an increasing rate, the sea-bottom pressure becomes larger than the hydrostatic pressure. This is noteworthy when we rapidly estimate a magnitude of tsunami by analyzing ocean-bottom pressure gauges deployed inside a focal region.

Keywords: tsunami, linear theory

## Envelope broadening of S-wave seismograms from earthquakes near the hypocenter of the 2011 Tohoku-Oki earthquake

Kazuya Hasegawa<sup>1\*</sup>, Ryota Hino<sup>1</sup>, Yoshihiro Ito<sup>1</sup>, Kensuke Suzuki<sup>1</sup>, Norihito Umino<sup>1</sup>

<sup>1</sup>Graduate school of Science, Tohoku Univ.

It is reported that the seismograms of the earthquakes in the forearc of the northeastern Japan show clear difference in their S-wave envelope shapes according to difference in their focal depths [Gamage et al, 2007; Koga 2010]. The seismograms of interplate earthquakes tend to have broader S-wave envelopes than those of intraplate earthquakes. We investigated the envelope broadening by measuring peak delay times of the S waves of earthquakes occurred beneath the landward slope of the Japan Trench. By including the aftershocks of the 2011 Tohoku-Oki earthquakes, we could analyze a number of intraplate earthquakes, both in the downgoing slab and in the overriding plate, as well as interplate earthquakes.

As a result, we noticed that interplate earthquakes are not always associated with significantly large peak delay times showing remarkable envelope broadening. In the trenchward half, up to ~ 130 km from the trench axis, of the landward slope area, the earthquakes near the plate interface tend to have evidently broadened S-wave envelope whereas those in the landward area are characterized by moderate peak delay times. We also confirmed that intraslab earthquakes have small peak delay times indicating less S-wave envelope broadening. Peak delay times of the earthquakes with considerable waveform broadening tend to increase rapidly in the small hypocentral distance range. This observation suggests strong short wavelength heterogeneity along the plate boundary in the trenchward zone. In contrast, increase rate of peak delay times of intraslab earthquakes are smaller than the averaged values. This reflects less heterogeneity in the Pacific slab in terms of short wavelength perturbation of material properties.

Keywords: S-coda wave, interplate earthquake, intraplate earthquake

## Time-lapse change in seismic velocity after the 2011 Tohoku-Oki earthquake estimated using ambient noise record

Ryota Takagi<sup>1\*</sup>, Naoki Uchida<sup>1</sup>, Tomomi Okada<sup>1</sup>, Toshio Kono<sup>1</sup>, Syuichi Suzuki<sup>1</sup>, Ryota Hino<sup>1</sup>, Akira Hasegawa<sup>1</sup>

<sup>1</sup>RCPEV, Graduate School of Sci., Tohoku Univ.

We detected temporal velocity change after the 2011 Tohoku-Oki earthquake using ambient noise interferometry. We used a seismic array in Iwate prefecture, which is equipped by Tohoku University. The array consists of 10 broadband sensors. Minimum and maximum separations of the array are 2.4 km and 18 km, respectively. Vertical component data of nine stations from January 2010 to December 2011 are used. After removing earthquake according to data amplitude, we computed normalized cross spectra for each day.

In the case of isotropic incidence of ambient noise, normalized cross spectra can be modeled by the Bessel function  $J_0(kr)$ , where  $k$  is the wavenumber and  $r$  is the separation distance [Aki 1957]. By fitting the Bessel function, we measured average phase velocity for each frequency. From average cross spectra before the earthquake, the phase velocities at 0.4, 0.8, 1.2 Hz are estimated as 3.183, 2.985, 2.878 km/s, respectively. After the earthquake, they are 3.176, 2.978, 2.863 km/s. Therefore, velocity decreases at 0.4, 0.8, 1.2 Hz are 0.22, 0.22, 0.52%, respectively. The phase velocities at other frequencies also show decrease after the earthquake. Especially, in the frequency range of 0.4-1.2 Hz, velocity decrease tends to be proportional to frequency.

The cross spectra for the case of anisotropic incidence of ambient noise also can be modeled by expanding the azimuthal distribution of incident wave amplitude in a Fourier series [Harmon et al., 2010]. When we modeled the noise source distribution by the fourth order expansion, the phase velocities at 0.4, 0.8, 1.2 Hz before the earthquake are 3.181, 2.980, 2.855 km/s, respectively. After the earthquake, the phase velocities are estimated as 3.173, 2.972, 2.842 km/s, which means velocity decrease by 0.24, 0.27, 0.46%.

Keywords: Seismic velocity change, Seismic interferometry, The 2011 Tohoku-Oki earthquake

## Ambient noise analysis using short-period seismometers and hydrophones

Takashi Tonegawa<sup>1\*</sup>, Yoshio Fukao<sup>1</sup>, Tsutomu Takahashi<sup>1</sup>, Koichiro Obana<sup>1</sup>, Shuichi Kodaira<sup>1</sup>, Yoshiyuki Kaneda<sup>1</sup>

<sup>1</sup>JAMSTEC

In the interferometry, the wavefield propagating between two positions can be retrieved by correlating ambient noise recorded on the two positions. This approach is useful for applying to various kinds of wavefield, such as ultrasonic, acoustic (ocean acoustic), and seismology. Off the Kii Peninsula, more than 150 short-period (4.5 Hz) seismometers, in which hydrophone is also cosited, had been deployed for ~2 months on 2012 by Japan Agency for Marine-Earth Science and Technology (JAMSTEC) as a part of "Research concerning Interaction Between the Tokai, Tonankai and Nankai Earthquakes" funded by Ministry of Education, Culture, Sports, Science and Technology, Japan. In this study, correlating ambient noise recorded on the sensors and hydrophones, we attempt to investigate characteristics of wavefield in the ocean, seafloor, and its solid-fluid interface.

The observation period is from Sep. 2012 to Dec. 2012. Station spacing is around 5 km. For 5 lines off the Kii Peninsula, the 30-40 seismometers are distributed at each line. Sampling interval is 200 Hz for both seismometer and hydrophone. The vertical component is just used in this study for correlation analysis. The instruments are located at 100-4800 m in water depth. In the processing for the both records, we applied a bandpass filter of 1-3 Hz, replaced the amplitude to zero if it exceeds a value that was set in this study, and took one-bit normalization. We calculated cross-correlation function (CCF) by using continuous records with a time length of 600 s, stacked the CCFs over the whole observation period.

As a result of the analysis for hydrophone, a peak can be seen in the CCF for pairs of stations where the separation distance is ~5 km. Although the peak emerges in the CCFs for the separation distance up to 10 km, it disappears in the case that two stations are greater than 15 km separated. As a next approach, along a line off the Kii Peninsula, we aligned CCFs for two stations with the separation distance of ~5 km, the peak emerged in the CCFs clearly shows a travel time variation as a function of water depth. The velocity of the signal is approximately estimated to be 1.2 km/s and 0.7 km/s at water depths of 2000 m, 4000m, respectively, and the velocity seems to gradually change between the two depths. In addition to the wave, a relatively weak signal can be seen, which shows a velocity of 1.4-1.5 km/s with no depth dependency.

As a result of the analysis for seismometer, a peak can be seen in the CCFs for two stations with a separation distance of ~5 km, which shows the water-depth dependent travel time as well as the analysis for hydrophone. However, the amplitude of the signal with a velocity of 0.7-1.2 km/s was weaker than those obtained in the analysis for hydrophone. In contrast, the signal with a velocity of 1.4-1.5 km/s emerged clearly compared to those using records of hydrophone. At present, no remarkable signals cannot be seen in the CCFs using horizontal components.

These signals obtained would be explained by the Stoneley wave, which has the largest amplitude at seafloor, the T-phase, which has the largest amplitude at the center of the SOFAR channel, the Rayleigh wave, which has the large amplitude within seawater and marine sediments, and also the superposition or coupling of these waves.

Keywords: Interferometry, Seafloor observation

## Cross terms of ground transfer function -generalization of Normalized Energy Density-

Hiroyuki Goto<sup>1\*</sup>

<sup>1</sup>Disaster Prevention Research Institute, Kyoto University

Normalized energy density (NED: Goto et al., 2011) is one of the essential quantities for a ground transfer function of a 1D layered structure model. This quantity is regarded as a type of norm for the power of the ground transfer function. The cross term of the functions is defined as an extension of the NED. The cross term is physically defined as the correlation coefficient between the two ground transfer functions. The cross term detects the harmony of two transfer functions; a finite value is obtained only in the case where peak frequencies coincide. The properties of the cross term is analytically proved for a two-layered case and numerically shown for three- and four-layered cases.

### Reference

Goto et al., Conserved quantity of elastic waves in multi-layered media: 2D SH case -Normalized Energy Density-, Wave Motion, 48, 602-612, 2011.

Goto, Fundamental property of cross terms of ground transfer function, Wave Motion, submitted.

Keywords: Normalized Energy Density, Ground transfer function, Cross term, Complex integration

## Improvement of SPAC method by taking the ratio of power spectra between two sites

XINRUI ZHANG<sup>1\*</sup>, Hitoshi Morikawa<sup>1</sup>

<sup>1</sup>Tokyo Institute of Technology

Since Aki proposed a new approach to estimate phase velocities of surface waves, spatial auto-correlation (SPAC) method has been a very useful tool to estimate ground structure because of its simple post-process. After that, many researchers both in and out of Japan continued to publish papers on practical adaption of Aki's theory to microtremor exploration. However, in all those improved methods, the layers under surface can only be assumed to be horizontal through the SPAC method while in fact, the layers are likely to be inclined slightly with certain angle. Hence, it is expected to obtain more detailed information of ground structure such as inclination by making better use of the records.

In recent years, the seismic interferometry theory has also been widely used to estimate ground structure. It is proved that in an elastic medium the Fourier transform of azimuthal average of the cross correlation of motion between two sites is proportional to the imaginary part of the exact Green's function between these sites. Hence, it becomes possible to calculate the ratio of imaginary part of different Green's function by taking the ratio of corresponding cross correlation to analyze ground

structure more particularly because Green's function indicates intrinsic property of the medium. Actually, seismic interferometry is conditionally consistent with the SPAC method which offers the base of introducing seismic interferometry to SPAC method.

SPAC method requires the multiplication calculation of Fourier transformation of records at two sites of center of an array and a one site on the circular array. By taking the ratio of power spectral between two different sites, it is hoped to obtain the ratio of imaginary part of Green's function according to seismic interferometry theory correspondingly and analyze the difference of ground structure through the ratio. More information such as the inclination of layers could be obtained.

Since this new concept has been proposed, some problems has been pointed out and the availability of the combination remains to be proved. Firstly, the ratio of power spectra is used to calculate the ratio of imaginary

part of Green's function which means the wavefield is supposed to consist of mainly body wave. However, the SPAC method requires the wavefield to be dominated by microtremors. It seems to be paradox but it is believed

that seismic interferometry theory itself satisfies wavefield of full wave. It is hoped that by taking the ratio of power spectra between two sites, the surface wave content will be extinguished and the body wave content remains.

Secondly, under the assumption of body wave being dominating, it is said that power spectra itself of each site could be used to analyze out the peak frequency of the ground structure (in simple case, the first layer) which tend to say that there is no need to take the ratio of them. Nevertheless, in wavefield dominated by microtremor and with the inclination of layers small enough, it is hard to extract useful information from each power spectra alone and to compare between them.

In this paper, the concept of SPAC method, interferometry and the combination of them are firstly proposed comprehensively. Then, in order to solve the two problems mentioned above, we use finite-difference method to

simulate some 2-layered simple layered medium under the wavefield dominated by microtrmors. Next, SPAC method is applied to certain array of observation sites to examine if this wavefield is effective for SPAC method. Finally, the availability of seismic interferometry would be analyzed and the need to take the ratio of power spectra will be shown.

Keywords: Power spectra, seismic interferometry, SPAC method, Green's function, layered medium

## Seismic interferometry imaging of seismograms observed in the Fujikawa-kako fault zone - ISTL seismic reflection survey

Yusuke Kawasaki<sup>1\*</sup>, Toshiki Watanabe<sup>1</sup>, Tanio Ito<sup>2</sup>, Ken-ichi Kano<sup>3</sup>, Yasutaka Ikeda<sup>4</sup>, Noriko Tsumura<sup>5</sup>, Kenji Nozaki<sup>5</sup>, Shintaro Abe<sup>6</sup>, Tetsuya Takeda<sup>7</sup>, Susumu Abe<sup>8</sup>, Akira Fujiwara<sup>8</sup>, Kazuya Shiraishi<sup>8</sup>

<sup>1</sup>Nagoya University, <sup>2</sup>Teikyo Heisei University, <sup>3</sup>Shizuoka University, <sup>4</sup>The University of Tokyo, <sup>5</sup>Chiba University, <sup>6</sup>AIST, <sup>7</sup>NIED, <sup>8</sup>JGI, Inc.

Seismic interferometry synthesizes the pseudo seismic response between receivers by cross-correlating records observed at the receivers, which corresponds to the seismic response observed at one receiver from the other receiver as a seismic source. The method enables us to obtain a subsurface structure using seismic records without using artificial sources.

The Fujikawa-kako fault system - Itoigawa-Shizuoka Tectonic line (ISTL) seismic reflection survey was conducted from April 2 to April 15, 2012. The survey line crosses the Fujikawa-kako fault zone, the Minobu fault system, and the ISTL. This survey aimed to elucidate the sedimentary structure of the lower Fujikawa River region, the deep structure of the fault system and the Philippine Sea Plate.

In this study, we applied the auto-correlation analysis and the cross-correlation analysis of seismic interferometry to the seismogram of natural earthquakes observed by the survey line. We compared the results obtained by seismic interferometry with the seismic reflection profile and evaluated the validity and the applicability of the methods.

We selected 24 earthquake records among the earthquake records observed during the reflection survey. The records of 8 artificial sources used for the wide-angle reflection survey were also used in this analysis. We extracted the P-wave of natural earthquake from the first arrival to S-wave arrival. For the analysis of the artificial source records, a time windows of 10 seconds from first arrival was applied. We applied the band pass filter between 4 and 16 Hz, and then, manually removed the traces with indistinct first arrival of P-wave before correlating each seismic record. Moreover, we applied the static correction, a technique often used in the analysis of a land reflection survey, to the reflection record to remove the effect of receiver elevation and shallow layers.

The result of the interferometry analysis using natural earthquakes and that using artificial sources shows good agreement. The profile is consistent with that of the seismic reflection survey. This indicated that seismic interferometry works as an effective exploration method. However, the deep structure, such as the plate boundary, was not well imaged in the profile. One of the reason is that the number of earthquake records used in this study was insufficient due to the short observation period.

Keywords: seismic interferometry, seismic reflection survey, subsurface structure, Fujikawa-kako fault zone, Itoigawa-Shizuoka tectonic line

## Seismic interferometry imaging of crustal structure using deep earthquakes in Tokai region

Mark Totani<sup>1\*</sup>, Toshiki Watanabe<sup>1</sup>, Koshun Yamaoka<sup>1</sup>, Aitaro Kato<sup>2</sup>, Takashi Iidaka<sup>2</sup>, Ryoya Ikuta<sup>3</sup>, Noriko Tsumura<sup>4</sup>, Makoto OKUBO<sup>5</sup>, Sadaomi Suzuki<sup>5</sup>

<sup>1</sup>Nagoya University, <sup>2</sup>The University of Tokyo, <sup>3</sup>Shizuoka University, <sup>4</sup>Chiba University, <sup>5</sup>Tono Research Institute of Earthquake Science

Seismic reflection survey using artificial sources is generally used as an imaging method of subsurface structure. By using the theory of interferometry, a subsurface structure can be imaged from seismic wave records of natural earthquakes as well as those of artificial sources. Imaging deeper structures is expected by using the natural earthquakes because the energy is larger than the energy from artificial sources.

This study aims to image the structures in the crust and the plate under the Tokai region by applying autocorrelation analysis (Claerbout, 1968) of seismic interferometry to the natural earthquake records observed by Tokai Array observation (Kato et al., 2010) from April to August, 2008. Records of the 8 Hi-net stations near the Tokai Array were also added.

Auto-correlation analysis assumes that the wave is at normal incidence since it stands in one-dimensional wave field. Therefore deep earthquake records (about 200 - 300 km) occurred in Pacific plate slab under the Tokai region were used. According to Kato et al. (2010), the deepest depth of Philippine Sea plate boundary is about 40 km under the Tokai region. From the theory of the Fresnel zone, it is estimated that the angle of incidence up to about 10 degree can be considered as normal incidence in the frequencies used for analysis. Therefore, deep earthquakes whose incident angle of 10 degrees or less in all stations were selected.

From the deep earthquake records of Tokai Array Observation that satisfy the condition of incident angle, we selected 11 events (Mj2.2 - 3.6) for the analysis. For Hi-net records, 40 events (Mj3.0 - ) of the deep earthquakes were extracted during 2004 - 2012. We used waves after P-wave arrival to S-wave arrival of the UD component as P-wave record and waves after S-wave arrival in the NS and EW components as S-wave. In prior to auto-correlation, pre-processing such as correction of the frequency response of seismometer, band-pass filter (pass band : 0.5 - 1.0 Hz) and deconvolution of source wave were applied.

In the result of analysis, we found continuous reflectors dipping NW near the depth of plate boundary shown in Kato et al. (2010). The reflectors were also found in the result of Hi-net data. Our preliminary interpretation is that the reflectors correspond to the plate boundary. The continuous reflectors were clear in the NW side of the array. However, it became obscure in the SE side. This may be due to the effect of sedimentary layers and the man-made noise in the SE side of the array. Also, this may be due to the regional geology because it seemed that the lateral change in the section locates near Median Tectonic Line and Butsuzo Tectonic Line.

We will apply the crosscorrelation analysis to the record in order to improve S/N ratio, and then, apply the same processes to teleseismic records.

Keywords: seismic interferometry, autocorrelation analysis, crustal structure, subsurface imaging, deep earthquake

## A split in the subducting Philippine Sea slab beneath the Izu-western Nankai collision zone

PADHY SIMANCHAL<sup>1\*</sup>, Takashi Furumura<sup>2</sup>, Takuto Maeda<sup>1</sup>

<sup>1</sup>ERI, the University of Tokyo, <sup>2</sup>CIDIR, the University of Tokyo

On July 5, 2011, an earthquake with a magnitude of 5.5 occurred off the Kii Peninsula in the northern Wakayama Prefecture in southwest Japan within the subducting Philippine Sea (PHS) plate at a depth of around 10 km. The earthquake caused strong shaking in the area near the epicenter. We analyzed the waveforms from this earthquake recorded at Hi-net and F-net stations in Japan. Such waveform analyses exhibit most of the earlier observations like dominance of low-frequency ( $f < 0.25\text{Hz}$ ) onset and following high-frequency ( $f > 2\text{ Hz}$ ) energy with long coda due to the stochastic waveguide effect of the subducting plate, proposed earlier by Furumura and Kennett (2005). Interestingly, we observed a clear difference in wave propagation pattern between east and west of the epicenter. For example, the waveforms for eastern part show S-coda are depleted with high frequency energy as compared to the western part. The duration of S-coda varies alternatively between high and low from east to west through center of the epicenter. The central stations show loss of low-frequency precursor to P-waves and presence of converted phases in P-coda. Such complexities in the observed waveforms are difficult to explain due to the radiation pattern of P- and S-waves and/or by anomalous propagation of seismic waves in existing plate model, indicating sudden lateral change in the wave guiding properties of the subducting slab, such as caused by the splitting of the slab as proposed by Ide et al. (2010).

To explain the observations, we employ two-dimensional finite-difference method (FDM) simulations of complete high-frequency P-SV wave propagation taking thinning of the PHS slab into account. In the plate model we included stochastic random heterogeneities described by exponential distribution function with a longer correlation length of 10 km in horizontal direction and much shorter correlation length of 0.5 km in depth and standard deviation from background P- and S-wave velocities of 5 % following the study of Furumura and Kennett (2007). We expect that the observed guided wave energy decouples from the waveguide where the slab is split. Low frequency energy leaks out of the slab in the low velocity mantle surrounding the slab. Taking into account the distribution of seismicity and focal mechanisms (Ide et al., 2010), and receiver function analyses (Shiomi et al., 2004) in the PHS plate, we expect a local velocity discontinuity or splitting of the plate at least to a depth of 30 km. Such a split in the PHS plate structure could also be manifested as non-volcanic tremor sources in the southwest Japan (Obara, 2002). The preliminary results, which suggest that the Philippine Sea slab is strongly split or partitioned beneath the Izu-western Nankai Trough in southwestern Japan, is the cause of the complicated waves from shallow inslab events. These effects need to be tested further with a 3-D FDM simulation employing high-performance computers with a variety of possible slab geometries. We finally discuss the implications of the new split plate model on the seismogenic potential of the area and the dynamics of the Nankai subduction in southwest Japan.

Keywords: Philippine Sea Plate, Scattering, Plate Tear, Wave Propagation

## T-waves from the nuclear test in North Korea

Masahiro Kosuga<sup>1\*</sup>

<sup>1</sup>Graduate School of Sci. and Tech., Hirosaki Univ.

North Korea conducted 3rd nuclear test on 12 February 2013. P-waves from the explosion were observed widely in the Japanese Island. We examined seismic T-waves observed by the seismometers of Hi-net stations because T-waves have been effectively used to detect explosions in the context of the Comprehensive Nuclear Test Ban Treaty (CTBT). We found that the T-waves were clearly observed in the Japan Sea side of northern Japan, while the waves are obscure along the coast from Yamagata to Fukuoka prefectures. This is probably due to the topography of ocean bottom. Along the paths of T-waves from the source to northern Japan the depth of ocean bottom is almost deeper than 3000 m. Thus there is few topographic high to prevent the propagation of sonic waves in the SOFAR channel. On the other hand, shallower and complex bathymetry causes incoherent arrival of T-wave energy along the paths to the southern Tohoku to Kyushu. We investigated the characteristics of T-waves by seismograms, envelopes, and spectrograms. At some stations in Hokkaido and northern Tohoku the amplitude of T-waves is much larger than P-wave. The peak frequency of T-waves reaches about 4 Hz. The most notable feature is the duration of T-waves; the duration is longer at stations in Hokkaido than at stations in northern Tohoku. Longer duration in Hokkaido is attributed to the contribution of reflected/scattered T-waves from the northern edge of the Yamato Bank situated at the middle part of the Japan Sea. Thus the T-waves from the nuclear test provide unique opportunity to investigate the lateral variation of the SOFAR channel and scattering characteristics of sonic waves in the Japan Sea.

**Acknowledgement:** We thank the National Research Institute for Earth Science and Disaster Prevention (NIED) for providing waveform data from Hi-net.

**Keywords:** T-wave, nuclear test, Japan Sea, topography, scattering, SOFAR channel

## Possibility of apparent velocity fluctuation caused by changes of the Hi-net instrument response

Tomotake Ueno<sup>1\*</sup>, Tatsuhiko Saito<sup>1</sup>, Katsuhiko Shiomi<sup>1</sup>, Yoshikatsu Haryu<sup>2</sup>

<sup>1</sup>NIED, <sup>2</sup>NIED/ADEP

Continuous seismograms recorded by Hi-net have been contributed to successful developments and applications of seismic interferometry analyses in which the temporal change of statistical properties of the seismograms are detected as a fractional change of subsurface structure. Because more than 10 years has passed since the Hi-net established, the instrument response could slightly change. The present study thoroughly analyzed the stability of the instrumental response for each Hi-net station and examine whether the change of the instrumental response can cause an artificial error in seismic interferometry analyses.

A record of instrument response by a calibration coil test is found at 9:00 a.m. in Hi-net. We determined the natural frequency  $f_0$  and damping parameter  $h$  by a grid search for the best fit between a theoretical instrument response and the observed one in time domain. The resolutions of this method for  $f_0$  and  $h$  were 0.05 Hz and 0.05, respectively. We obtained a temporal change of the  $f_0$  and  $h$  for about 10 years for each station. The variations were within the resolution of the grid search method. We obtained small  $f_0$  shifts approximately 0.02 Hz at KMIH (Kamaishi, a station located near the coast in Iwate) seismic station at the 2011 Tohoku-oki earthquake. A very small and long term trend of instrument response is also recognized for the period.

In order to investigate influences of the changes of instrument responses on seismic interferometry analysis, we calculated various waveforms using the  $f_0$  and  $h$  with a range of 0.9 - 1.1 Hz and 0.6 - 0.8, respectively. A velocity fluctuation corresponding to these instrumental response variation, or apparent velocity fluctuation, was estimated by a stretching method of auto-correlation-function (ACF) after a band-pass filter of 1 - 3 Hz and 1 bit normalization were adapted, where reference ACF was calculated with  $f_0 = 1$  Hz and  $h = 0.7$  as typical Hi-net instrument parameters. As a result, small apparent velocity changes less than 0.1 % were obtained corresponding to the shifts of the instrument responses. Because this change is significantly smaller than those typically reported as a subsurface velocity change (for example, more than 0.3 % velocity decrease was found by Ueno et al., 2012), we concluded that the Hi-net instrument responses are stable enough to detect subsurface velocity change  $> 0.1$  % by seismic interferometry analyses.

Keywords: Hi-net, instrument response, seismic interferometry, apparent velocity change

## An attempt to detect seismic velocity change due to tidal strain based on autocorrelation analysis of ambient noise

TAKANO, Tomoya<sup>1\*</sup>, NISHIMURA, Takeshi<sup>1</sup>, NAKAHARA, Hisashi<sup>1</sup>, TANAKA, Sachiko<sup>2</sup>

<sup>1</sup>Department of Geophysics, Graduate School of Science, Tohoku University, <sup>2</sup>NIED

Recent studies using noise correlation method report temporal changes in seismic velocity associated with occurrence of large earthquakes and volcanic activities or seasonal variations (e.g. Titi et al., 2012; Hobiger et al., 2012). These temporal changes of the structure can be interpreted as the damage in near surface due to strong motion or the static stress change due to coseismic slip on the fault or volcanic crustal deformation. A few field experiments of in situ seismic velocity measurements detected seismic velocity changes of 0.1%~0.5% due to tidal strain (e.g. Reasenberg & Aki, 1974; Yamamura et al., 2003). In frequency band, these active experiments using piezoelectric transducer or air gun as sources with dominant frequency of 1kHz or 30 Hz are not always consistent with seismic interferometry which have reported temporal changes. Using dilation and compression by tidal force as an external force, we examine seismic velocity changes due to applied stress based on autocorrelation function (ACF) analysis of ambient noise.

We use the vertical component of continuous seismic data (100Hz sampling) at 118 Hi-net stations in the northeastern Japan from 1 January to 31 December 2010. To remove signals from natural earthquakes, we use data with amplitudes less than a threshold value, which is set to be five times the median of 1 year RMS calculated every 10 min, and apply one-bit normalization. The data is filtered at frequency band of 1-2Hz, 2-4Hz. ACFs are calculated every 10 minutes.

To detect small velocity changes due to tidal stress in 103 Pa order, we need to select data in relatively calm day. We measure time delays by applying cross correlation analysis for the mean ACF in 2010 and daily ACFs. Correlation coefficients and time delays are calculated by shifting a time window of 2.56 s during the lag time of 1.28-10 s. For a homogeneous medium in which seismic velocity constantly increases or decreases, we estimated daily seismic velocity changes from the relation between lag time and delay time. In order to enhance the temporal resolution of the CCF, we interpolate with a sampling frequency of 800 Hz.

We compute tidal synthetic volumetric strain at each station using GOTIC2 program (Matsumoto et al., 2001) in estimated calm days. We define tidal strain with a value more than  $5.0 \times 10^{-9}$  and less than  $-5.0 \times 10^{-9}$  as dilational and compressional episodes respectively, and we stack ACFs in each period. We call the ACF stacked in dilational episode DACF and that in compressional episodes CACF. We estimate the time delay of DACF for CACF only when the correlation coefficient is larger than 0.99.

Focusing on seismic velocity changes obtained stably, we select stations which estimated error of seismic velocity changes is smaller than 0.01%. At the frequency band of 2-4 Hz, we measure seismic velocity changes at 27 stations, and summarize them in a histogram. Velocity changes are distributed in  $-0.06 \pm 0.06\%$ , and the peak shows  $-0.01\%$ . It can be thought that seismic velocity decrease in dilation, our result may show velocity changes due to tidal strain. However the weighted average of seismic velocity changes is estimated  $-0.006 \pm 0.005\%$ , which show our methods cannot always give meaningful result. On the other hand, at the frequency band of 1-2 Hz, we measure velocity changes at 45 stations. At this frequency band, velocity changes are distributed in  $-0.14 \pm 0.09\%$ , and the weighted average of seismic velocity changes is estimated  $0.0 \pm 0.004\%$ . These results may show that our method cannot detect seismic velocity changes due to tidal stress.

In comparison with previous studies, we cannot detect clear seismic velocity changes corresponding to tides. There may be difference of frequency band between previous study and our study as a cause, so we will analyze at higher frequency band.

### Acknowledgments

I thank NIED for making continuous data of the Hi-net available.

Keywords: seismic interferometry, autocorrelation function, ambient noise, earth tide, temporal seismic velocity change

## Validation of S-wave velocity structure in the southern Kanto based on Green's functions with seismic interferometry

Kosuke Chimoto<sup>1\*</sup>, Hiroaki Yamanaka<sup>1</sup>

<sup>1</sup>Tokyo Tech

Seismic interferometry is known to provide Green's functions between the stations pairs by using the long-term microtremors obtained at both stations. Surface-waves are expected to be dominant in the Green's functions from microtremors observations on the earth surface. Since surface-waves provide the information about the near surface structures, we use Green's functions estimated with seismic interferometry for validation of the S-wave velocity structures in the southern Kanto.

We have constructed the network for long-term microtremors observation in the southern Kanto, and applied it to seismic interferometry. We have also estimated the S-wave velocity structures with tomographic inversion based on the slowness of the cross correlation functions. Recently, the amplitudes of cross correlation functions are also studied to reconstruct the amplitude of Green's function (e.g. Tsai, 2011; Prieto et al., 2009). Seismic interferometry is often applied to the microtremors of which amplitudes are normalized to 1 bit (Campillo and Paul, 2003) or with threshold clipping (Shapiro and Campillo, 2003). However, these procedures distort the amplitudes of microtremors and the distortion of the amplitudes of reconstructed Green's functions, accordingly. Chimoto and Yamanaka (2012) used the data processing by Prieto et al. (2011), which applies no normalization for microtremors, and showed the possibility in the use of the information about the amplitudes. They also demonstrated to obtain the appropriate signals of Green's functions from the cross correlation with the data processing.

In this study, we also used the data processing denoted by Chimoto and Yamanaka (2012) to use the information about the amplitude of Green's functions. Since surface-waves of Green's functions of which amplitudes preserved provide the useful information about the near surface structure, we use them to validate the S-wave velocity structures in the southern Kanto. We compare the estimated Green's functions with seismic interferometry and the theoretical Green's functions from the empirical S-wave velocity models proposed by Yamanaka and Yamada (2006) to validate it.

In the southern Kanto plane, where the dense microtremor array observation has been conducted, the appropriate S-wave velocity structures would have been estimated, because both Green's functions show the similarity. However, there also existed the difference in the later phases due to the scattering in the short period range, indicating that the further modification of the models is needed. We then focus on Sagami bay and Tokyo bay, because the model is still unknown due to the difficulty of conducting the geophysical exploration. We found that both Green's functions had difference and show the complexity due to the complexity of the subsurface structures in such areas. The difference in Green's functions was not only in direct wave but also in later phases. The difference was significant in the short period range. This suggests that the further modification of the models is required in such areas.

Keywords: Seismic interferometry, Green's function, S-wave velocity structure, Southern Kanto, Cross correlation function, Microtremor